Journal of Biological Rhythms

http://jbr.sagepub.com

Arrhythmic Rats after SCN Lesions and Constant Light Differ in Short Time Scale Regulation of Locomotor Activity

Juan José Chiesa, Trinitat Cambras, Ágata Rita Carpentieri and Antoni Díez-Noguera

J Biol Rhythms 2010; 25; 37
DOI: 10.1177/0748730409352843

The online version of this article can be found at:
http://jbr.sagepub.com/cgi/content/abstract/25/1/37

Published by:
SAGE
http://www.sagepublications.com

On behalf of:

Society for Research on Biological Rhythms

Arrhythmic Rats after SCN Lesions and Constant Light Differ in Short Time Scale Regulation of Locomotor Activity

Juan José Chiesa,[*] Trinitat Cambras,[†] Ágata Rita Carpentieri,[†,1] and Antoni Díez-Noguera[†,2]

[*]*Departamento de Ciencia y Tecnología, Universidad Nacional de Quilmes–CONICET, Bernal, Argentina, and* [†]*Departamento de Fisiologia, Facultat de Farmàcia, Universitat de Barcelona, Barcelona, Spain*

Abstract Circadian rhythm disruption (i.e., arrhythmicity) in motor activity is an abnormal behavioral pattern. In rats, it can be caused by the lesion of the hypothalamic suprachiasmatic nucleus (SCN) and by prolonged exposure to constant light (LL). We carried out a comparative study of these arrhythmic phenotypes to assess the role of the SCN in the regulation of the motor output beyond circadian rhythmicity. Motor activity series were studied in rats that had become arrhythmic as a result of 1) LL exposure at 2 light intensities: 300 lux (LL_{300}) and 1.3 lux ($LL_{1.3}$), and 2) SCN lesion (SCNx). The Fourier spectra, the fractal Hurst coefficient (*H*) from the autocorrelation function, and the β slope from the power spectral density were calculated in data sections at baseline, when the rats were still rhythmic, and later at stages with undetectable circadian rhythms. In the LL_{300} group, high power content was detected at frequencies of 8 to 4 h (i.e., ultradian). Lower power content for these harmonics was found in the $LL_{1.3}$ group, whereas no dominant harmonics appeared in the SCNx group. Independently of the manifestation of circadian rhythm, *H* values were higher and more sustained in time in rats exposed to LL_{300} but gradually decreased in rats exposed to $LL_{1.3}$. Fractal correlation was found in control DD group but was absent in the SCNx group. We conclude that scale-invariant regulation of the motor pattern by SCN activity is dependent on light intensity but independent of the circadian rhythm output. Adjusting the light intensity by modifying the coupling degree between the population of oscillations could affect the dynamics of each individual oscillator in the SCN, making it less predictable.

Key words circadian, arrhythmic behavior, fractal analysis, scale invariance, suprachiasmatic

Virtually all physiological and behavioral processes are controlled by a circadian clock, which in mammals is located in the suprachiasmatic nucleus (SCN) of the hypothalamus. Classically, the SCN has been subdivided into dorsomedial and ventrolateral regions, based initially on retinal innervation patterns,

1. Current address: Cátedra de Bioquímica y Biología Molecular, Facultad de Ciencias Médicas, Universidad Nacional de Córdoba–CONICET, Córdoba, Argentina.

2. To whom all correspondence should be addressed: Antoni Díez-Noguera, Departamento de Fisiologia, Facultat de Farmàcia, Universitat de Barcelona, Barcelona, 08028 Spain; e-mail: adieznoguera@ub.edu.

JOURNAL OF BIOLOGICAL RHYTHMS, Vol. 25 No. 1, February 2010 37-46
DOI: 10.1177/0748730409352843

and later on the observation that these regions are defined by phenotypically distinct cell types (Antle and Silver, 2005). These subregions differ in their cytoarchitecture, connectivity, topography, and histochemistry (Leak and Moore, 2001; Moore et al., 2002). Moreover, low-density SCN cultures contain single-cell neuronal oscillators capable of generating circadian rhythms of electrical activity (Welsh et al., 1995) and gene expression (Yamaguchi et al., 2003). Thus, intercellular communication mechanisms are necessary in the SCN to act in vivo as a tissue clock with coherent circadian outputs. Examples of these mechanisms include voltage-gated Na^+ channel–dependent action potentials (Yamaguchi et al., 2003) and electrical (Long et al., 2005) and chemical (Maywood et al., 2006) synapses.

Most 24-h output rhythms are immediately abolished by lesions in the SCN (SCNx) (Stephan and Zucker, 1972; Eastman et al., 1984), resulting in arrhythmic behavioral patterns. In rats, arrhythmicity may also develop following chronic exposure to bright light (LL), which gradually disrupts the circadian outputs until complete arrhythmicity is reached (Eastman and Rechtschaffen, 1983; Depres-Brummer et al., 1995). In addition, a single light pulse delivered under constant darkness at a specific time of the subjective night has also been reported to result in the persistent lack of circadian rhythms in the Siberian hamster (Steinlechner et al., 2002) and in *Drosophila* sp. (Winfree, 1971).

According to these findings, circadian arrhythmicity is a state that can result not only from the absence of the SCN clock but also following the manipulation of lighting conditions, which can disrupt the functioning of the pacemaker. To date, 2 theories have been proposed to explain circadian arrhythmicity: 1) that light stops a single pacemaker by displacing the system towards its singularity (i.e., the point along the phase plane at which all circadian phases converge) (Winfree, 1971; Pittendrigh et al., 1981a), and 2) that mutual coupling is lost in multiple circadian oscillators, resulting in scattered individual phases (Pittendrigh et al., 1981b). Studies in mice have shown that prolonged exposure to LL induces behavioral arrhythmicity, which correlates with the desynchronization of cellular oscillators in the SCN (Ohta et al., 2005). Based on this, the latter theory explaining circadian arrhythmicity is therefore more likely.

Recent studies in rats have shown that an SCN lesion not only abolishes both circadian and ultradian rhythms but eliminates the scale-invariant properties (fractal) of each motor activity (Hu et al., 2007) as well as heart-rate fluctuations (Hu et al., 2008). Specifically, it was shown that the SCN lesion in rats abolished scale-invariant patterns over a period of between 4 and 24 h and significantly altered the patterns in less than 4 h. This indicates that the SCN participates in a control scheme across a wide range of time scales. Scale-invariant patterns are present in various physiological processes, such as heartbeat (Peng et al., 1995), breathing (Fadel et al., 2004), and gait (Goldberger et al., 2002).

Although the SCN has been proposed as being a major control node for the regulation of patterns along multiple time scales, the environmental lighting modulation of this fractal behavior has not yet been assessed to date. In this work, we studied the motor activity pattern of rats that had become arrhythmic as a result of SCNx or after being exposed to chronic LL at 1 of 2 different intensities: 300 lux (LL_{300}) and 1.3 lux ($LL_{1.3}$). We have also included a group of rats with normal circadian regulation kept under constant darkness (DD). Time series were compared using conventional circadian rhythm analyses methods, as well as complex and fractal analyses. Even when subjects did not exhibit circadian rhythms, detecting the temporal fractal correlation under the different experimental conditions allowed us to draw conclusions about the SCN regulation of motor activity and the modulation of SCN oscillators by light.

MATERIALS AND METHODS

Animals and Behavioral Recording

Four-month-old male Wistar rats (Charles River Laboratories, Les Oncins, France) were housed in the institution's animal facilities to allow them to acclimatize. They were then kept in isolation in transparent 25 × 25 × 12-cm methacrylate cages and transferred to sound-proof and temperature- and humidity-conditioned (20-22 ºC, 50%-80%) chambers. Animals were fed with food pellets (Panlab A04, Barcelona, Spain) and tap water *ad libitum*, and their cages were supplied with wood chippings for bedding, which was renewed weekly. The general spontaneous motor activity of each animal was measured throughout the experimental procedures using an activity meter that included 2 perpendicular infrared beams, which crossed the cage 7 cm above the floor. Activity counts were sampled and stored on a computer hard disk using time frames of 1 min.

Experimental Procedure

For control, we used 10 rats with normal circadian regulation, exposed to DD conditions (less than 0.5 lux, red light) for 2 months (DD group). The experimental rats suffered behavioral arrhythmicity as a result of one of the following methods:

1) Exposure to constant light (LL): A) Fifteen rats were exposed to indirect bright white light from two 36-W fluorescent tubes (main peaks at 450 nm, 550 nm, and 650 nm) of about 300 lux of intensity for approximately 2 months (group LL_{300}); B) Ten rats were exposed to indirect dim white light from light-emitting diodes (main peak at 470 nm and a wider one at 570 nm) of about 1.3 lux for approximately 2 months (group $LL_{1.3}$). In both scenarios, a period of approximately 2 months was necessary to accurate detect a persistent lack of a circadian rhythm in the animals.

2) SCN lesion (SCNx): Thirty rats were kept under constant darkness (~0.1 lux red lighting, DD) until the day of the surgery (approximately 15 days). When creating the lesions in the animals, surgery was performed under a mix of ketamine (75 mg/kg) and xylazine (10 mg/kg) anesthesia. Animals were placed inside a stereotaxic instrument (model 900, David Kopf Instruments, Tujunga, CA), and the tip of the electrode was lowered to the SCN region (–1.3 mm posterior to the bregma; 9.2 mm below the skull) (Paxinos and Watson, 1998). The electrode transmitted a radio frequency from a lesion generator system (model RFG-4A, Integra Radionics, Burlington, MA), which damaged the tissue using heat (~90 °C, 1 min). The rats were then moved to the recording chambers, where they were kept under DD.

Circadian Analyses

Raw data were accumulated in 15-min intervals for all the analyses. Double-plotted actograms at modulo 24 h in parallel with periodograms using the χ^2 method (Sokolove and Bushell, 1978) were calculated to determine the absence of circadian periodicity, using consecutive data sections with a length of 10 days (stages for the analyses, s_i). The scanning range for the periodogram was from 1 h to 26 h, and the level of significance was $p = 0.05$, with Bonferroni correction for multiple estimations. The criteria used to define arrhythmicity were the permanent absence of a significant circadian peak (range, 22-26 h) in the periodogram along the different stages (Figure 1). The use of this criterion implies that we did not use for the analysis those animals that, although they were arrhythmic, showed a sporadic peak in the circadian range in some stage. With this criterion (no circadian rhythm in none of the 4 stages), we selected 10 SCNx, 4 LL_{300}, and 4 $LL_{1.3}$ rats. The baseline for each rat was considered the 10 days, at the beginning of the experiment, under the same light intensity, in which the animals still showed a clear circadian rhythm.

In rats with arrhythmicity, a daily serial spectral (Fourier) analysis was applied to the first 10-day data section. Thus, the spectral decomposition for each consecutive 24-h subsection was obtained, which allowed us to compose a description of the harmonic components along the 10-day section. The spectral analysis was calculated with 25 harmonics, with the fundamental harmonic (H_1) being a rhythm of a 24-h period. The rhythms of the remaining harmonics (H_i) had submultiple periods of 24/2 h, 24/3 h, 24/25 h, etc., respectively. In this way, an array of ultradian periodicities, from the second 12-h period harmonic (H_2) to the 25th (H_{25}), of near 1 h was covered. We obtained the power content (PC) for each H_i expressed as the percentage of variance (%Var), explained by a given H_i with respect to the total variance in the time series. Individual power spectra were averaged for each group and represented using a gray scale in graphic matrixes, structured using harmonics (columns) and days (rows) (Figure 2A). In addition, the serial PC values corresponding to each H_i were averaged for the 10-day section, and then the means and standard errors (SEMs) for each group were represented (Figure 2B).

Complex and Fractal Analyses

Fractal analysis was performed in all cases with individual time series from the consecutive 10-day stages. These were included for this analysis, a baseline stage, s_1, when the rats still had a circadian rhythm, followed by consecutive stages s_2-s_5, with clear arrhythmicity. In the case of SCNx rats, s_1 corresponds to days prior to the lesion. Fractal measures were used to calculate the extent of scale invariance in the motor patterns. These methods are based on obtaining the relationship between the logarithm of any statistical feature of the process (F(n)) and the logarithm of the scale (n) from which it was obtained (Eke et al., 2002). A power-law function indicates scale invariance, defined by a straight line on the log-log plot of F(n) versus scale, yielding $F(n) \sim n^{\alpha}$, where α is the scaling exponent that quantifies the interval correlation in the time series. This analysis was carried

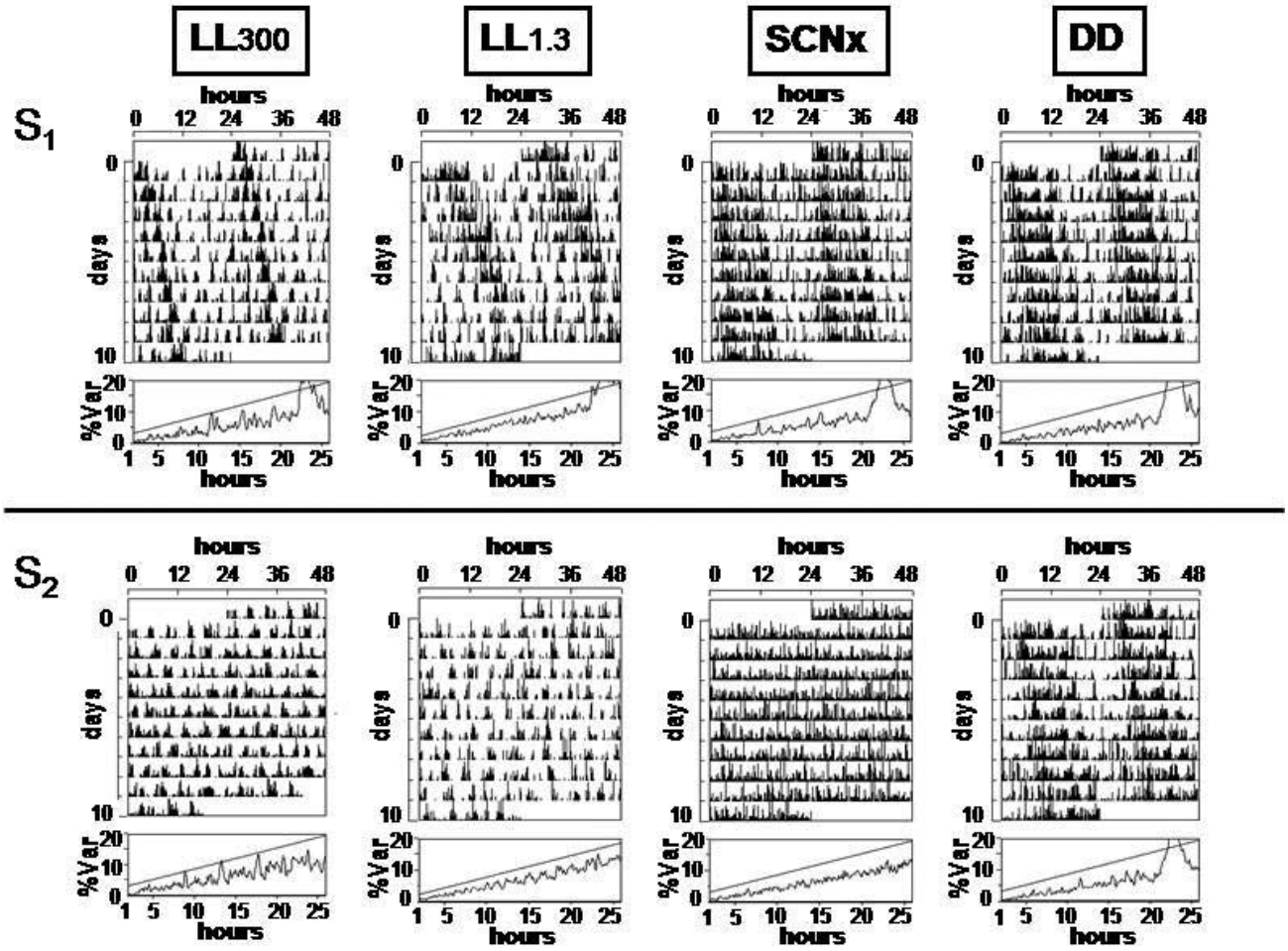

Figure 1. Actograms double plotted at modulo 24 h of representative rats showing circadian arrhythmicity in LL_{300}, $LL_{1.3}$, and SCNx groups. One rat from the DD control group is also represented. Graphs at the top correspond to the baseline stage (s_1), when animals were still rhythmic, while those at bottom show the first 10-day stage (s_2) with no dominant circadian period. Scale was defined from zero to the 95% percentile of data maximum. Graphs below actograms correspond to χ^2 periodograms of the data above, showing the %Var calculated for a range from 1 to 26 h. The line depicts significance level ($p = 0.05$) for the statistical estimation of periods. Note that significant circadian peak (about 35 %Var) in the DD group is out of graph scale.

out on both the frequency and time domains, by the calculation of power spectral density (PSD) and the autocorrelation function (Ac), respectively.

To accurately evaluate the nature of the time series (fractional Gaussian noise, fGn, or fractional Brownian motion, fBm, and the "color" of the noise), the β slope on the log-log plot of PSD was estimated. PSD calculated the power content of each harmonic in absolute values by taking measurements from the fundamental 24-h harmonic to the Nyquist frequency (N/2: 30-min harmonic). In this way, estimates for the slope of the regression line were done on the log(PC) versus log(H_i) relationship (i.e., spectral index, β) using the improved version of PSD, $^{low}PSD_{we}$ (Eke et al., 2000). According to this method, after detrending and parabolic windowing, the fitting range to estimate β uses the whole PSD but excluding frequencies $f>1/8$ of maximal frequency (equivalent to a period of 240 min), indicating fGn noise if $-1<\beta<1$, and fBm if $1<\beta<3$ (Eke et al., 2000; Delignieres et al., 2006).

Following this, Ac was calculated to determine the time correlation within each series, which allowed us to know the extent to which the value of a given event depends on previous values (i.e., memory of the process). To achieve this, the correlation coefficient was obtained using data lags from 1 to N/2 in the consecutive stages. The Hurst coefficient ($1>H>0$) was calculated from the first value (r_1) of the autocorrelation function using the formula $H = (\log_2(r_1 + 1) + 1)/2$, deduced from the equation $r_1 = 2^{2H-1} - 1$ (van Beek et al., 1989) as described in Eke et al. (2002). The

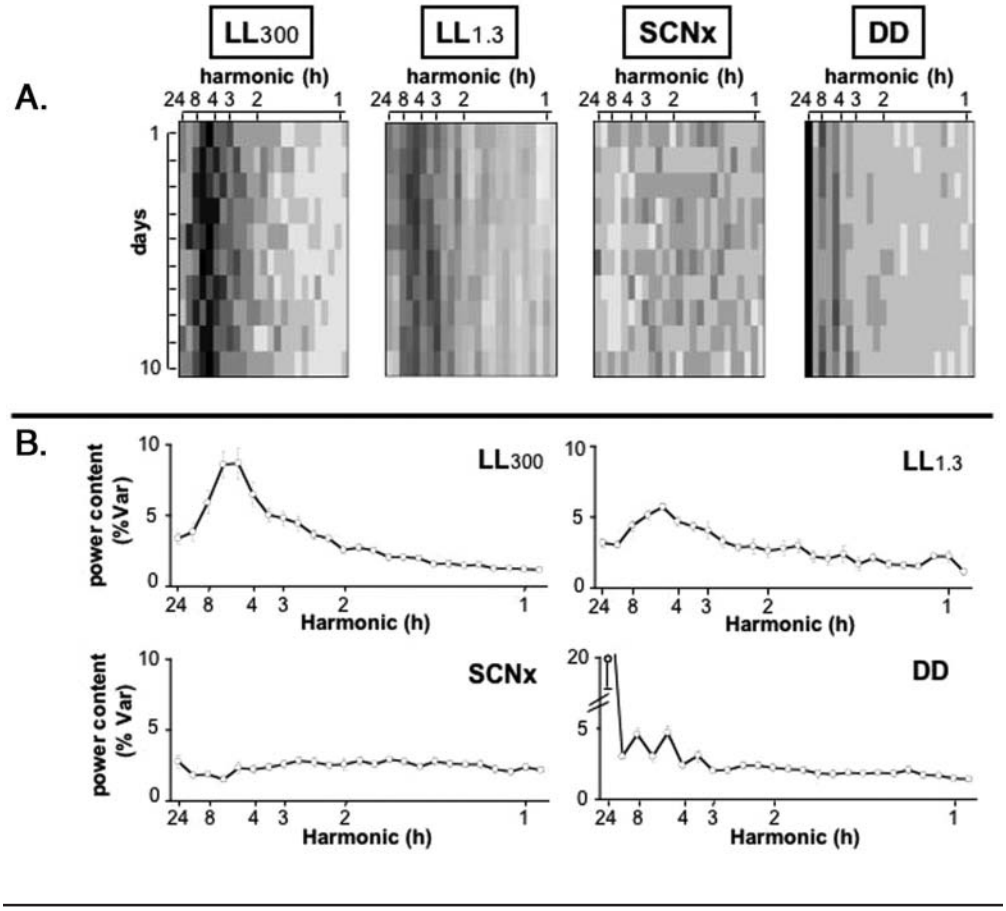

Figure 2. Daily spectral decomposition obtained with the Fourier analysis in time series. (A) Each graph corresponds to the mean graphic matrix of each group, obtained by averaging the serial analysis of the first 10-day stage lacking circadian period, for each animal. Matrixes represent PC values (%Var) of the successive 25 harmonics (columns) calculated for each consecutive day (rows). Each harmonic is indicated by the corresponding period expressed in hours (top of each graph). Values are represented on a gray scale, with black being the highest (10 %Var). (B) Mean ± SEM PC values of the harmonics calculated for the whole 10-day segment for each group. Note that scale for PC in the DD group is truncated to include H_1 = 20 %Var.

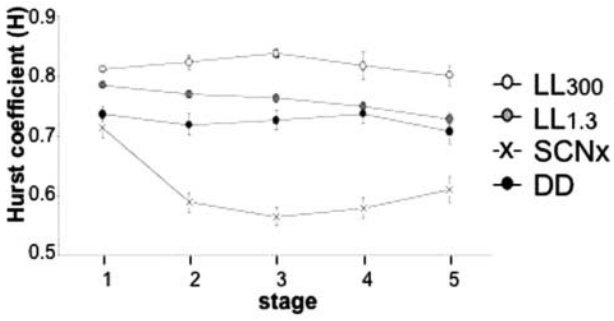

Figure 3. Mean ± SEM values of the Hurst coefficient obtained for each group calculated separately for all the consecutive stages. Dotted line separates the stage (s_i) when the rats still manifested a circadian period, from the stages with sustained arrhythmicity (except for control DD group, which was always rhythmic).

closer H is to 1, the longer is the memory of the process. In general, positive correlation corresponds to values of H ranging from 0.5 to 1. H = 0.5 denotes no correlation at all and corresponds to a pure Gaussian process (random white noise). When H < 0.5, the signal shows anticorrelation. The point at which correlation fell below the limit of statistical significance in the log-log plot (t_c) is also reported, which offers an estimation of the correlation time (i.e., the memory of the process). In addition, H was calculated for the difference series ($y_i = x_i - x_{i-1}$) to confirm the Gaussian nature of the time series. This was achieved by checking for a reduction of *H* of approximately 0.5 in the difference series (y) when compared with the original raw data (Eke et al., 2000).

To describe the time-dependent changes, *H* was calculated and reported in 4 consecutive stages (a total of 40 days with arrhythmicity) for all the groups. We also included the previous corresponding paired value, which was obtained when the animal still had a circadian period (Figure 3). t_c and β were reported only for this first stage and the following one lacking this rhythmicity. All the values were reported as mean ± SEM. Multiple-variable ANOVA (MANOVA) was used to assess which H_i PC variable significantly differed between the groups. A 2-way ANOVA was used to compare fractal measures, with the stages (s_i) and groups as factors. A Tukey test, applied to either equal or unequal samples, was used for post hoc comparisons. Differences were considered significant at $p < 0.05$.

Table 1. Fractal analysis obtained from $^{low}PSD_{we}$ (β spectral index) and Ac (*H* and t_c).

	β		*H*		t_c (min)	
	s_1	s_2	s_1	s_2	s_1	s_2
LL_{300} $n = 4$	–0.55 ± 0.06	–0.45 ± 0.04	0.81 ± 0.01	0.82 ± 0.02	68.3 ± 9.6	70.8 ± 5.0
$LL_{1.3}$ $n = 4$	–0.53 ± 0.08	–0.51 ± 0.08	0.79 ± 0.01	0.77 ± 0.01	52.6 ± 3.4	45.1 ± 2.4
SCNx $n = 9$	–0.38 ± 0.04	–0.05 ± 0.03	0.71 ± 0.02	0.59 ± 0.02	41.9 ± 2.0	26.6 ± 1.1
DD $n = 9$	–0.50 ± 0.04	–0.59 ± 0.05	0.74 ± 0.01	0.72 ± 0.02	46.5 ± 1.9	43.9 ± 3.5

Values are expressed as the mean ± SEM calculated for the groups in stage s_1 (when all rats still exhibited a circadian period) and in s_2 (when all rats, except DD, showed no circadian rhythm).

The experimental protocols used here were approved by the Institutional Animal Care and Use Committee of the University of Barcelona, in agreement with the recommendations of the Federation of European Laboratory Animal Science Associations.

RESULTS

Circadian Analyses

Double-plotted actograms at modulo 24 h shows data section at baseline (s_1) and the following with confirmed lack of a circadian rhythm in animals from each group (s_2). This arrhythmicity is demonstrated both in the actogram and by the absence of a significant circadian peak in the periodogram, normally found in the control DD group (Figure 1). Despite this, visual inspection of the actograms revealed different temporal patterns when comparing arrhythmic rats. Clustered activity bouts were seen in the LL_{300} lux group. In contrast, more diffused bouts were seen in the SCNx group. Rats from the $LL_{1.3}$ lux group showed, to the same extent, an intermediate phenotype with respect to the LL_{300} and SCNx groups.

A spectral breakdown of the time series in the range of 24 h to approximately 1 h revealed clear differences among the groups. Figure 2A shows the mean power spectra calculated for consecutive 24-h periods in each group. Greater PC values represent a higher percentage of variance associated with the harmonics. A marked band of ultradian frequencies, from approximately the third to the sixth harmonic (8-4 h), was observed in the LL_{300} group, which was sustained throughout the 10-day period (Figure 2A). In addition, harmonics from the fourth to the sixth (6-4 h) were present in the serial analysis of the $LL_{1.3}$ group but to a lesser extent. In contrast, a flattened spectra lacking any dominant harmonic was seen in the SCNx group, while the control rats under DD conditions showed a typical spectrum with a high PC of 24 h, together with unusual harmonics caused by the squared waveform.

The 24-h harmonic was clearly diminished in the 3 arrhythmic groups, and no differences were observed between them. These changes were also seen in the mean spectra obtained from the serial analysis (Figure 2B). The results of the MANOVA analysis revealed significant differences in the PC between the 4 groups ($p < 0.001$), which were greatest in the following harmonics: H_1 ($p < 0.001$, DD v. all groups); H_2 ($p < 0.01$, LL_{300} v. SCNx); H_3 ($p < 0.001$, LL_{300} v. SCNx; $p < 0.05$, DD v. SCNx); H_4 ($p < 0.001$, LL_{300} v. SCNx and DD; $p < 0.05$, $LL_{1.3}$ v. SCNx); H_6 and H_8 ($p < 0.001$, LL_{300} v. SCNx and DD); H_5 ($p < 0.001$, LL_{300} v. SCNx; $p < 0.05$ v. DD); H_7 ($p < 0.001$, LL_{300} v. SCNx; $p < 0.05$ v. DD); and H_9 ($p < 0.05$, LL_{300} v. SCNx; $p < 0.001$ v. DD). These results indicate a higher ultradian band for LL_{300} versus SCNx (from 12-3 h), while no differences were observed below the 2.6-h frequency.

Fractal Analyses

All β values obtained in the $^{low}PSD_{we}$ analysis were lower than 1, indicating that the motor activity series could be considered as fGn (Table 1). Thus, H was calculated directly from the Ac function applied to the raw data. The fGn nature of the process was also confirmed by the fact that *H* calculated from the difference series had values of approximately 0.5 units below those found in the raw data (Table 1).

The *H* coefficient obtained from Ac changed over time in a different way depending on the experimental conditions (Figure 3). Firstly, rats maintained in LL_{300} conditions maintained the same high values as the baseline, even when they still had circadian rhythmicity (s_1) towards the end of the protocol (s_5). In contrast, *H* values obtained from the $LL_{1.3}$ group, which were also arrhythmic, gradually decreased over time. Rats that were exposed to SCNx showed an abrupt drop from the baseline *H* values (s_1) as soon as they became arrhythmic (s_2). Finally, a stable *H* value was observed in free-running rats with endogenous circadian regulation (DD group) during all stages. The 2-way ANOVA analysis produced

statistically significant differences for the stage ($p < 0.001$), the groups ($p < 0.001$), and the stage-group interaction ($p < 0.001$). While the stage effect did not influence the *H* values in the LL_{300} or DD groups, it produced significant differences in the $LL_{1.3}$ group ($p < 0.01$), which were higher for s_1 versus s_4 and s_5 ($p < 0.05$) and for s_2 and s_3 versus s_5 ($p < 0.05$). In addition, in the rats exposed to SCNx, the *H* coefficient was statistically different ($p < 0.001$); it was higher for s_1 ($p < 0.01$) versus the remaining stages.

When comparing groups within the stages, we found significant differences between the groups ($p < 0.001$). LL_{300} had significantly higher values of H than SCNx in all stages ($p < 0.001$) and was significantly higher than DD in s_1, s_3 ($p < 0.001$) and s_2, s_4 ($p < 0.01$). $LL_{1.3}$ had higher values than SCNx in s_2, s_3, s_4 ($p < 0.001$), and s_5 ($p < 0.01$), while DD was higher than SCNx in s_2, s_3, s_4 ($p < 0.001$). Comparable results were found for t_c values describing the time of correlation (Table 1). The 2-way ANOVA revealed significant differences in the stage ($p < 0.05$) and group ($p < 0.001$) comparison. Although stage alone resulted in significant differences only for SCNx ($p < 0.001$), the analysis for the influence of groups resulted in significant differences in s_1 ($p < 0.001$), with LL_{300} being higher than SCNx and DD ($p < 0.001$), as well as in s_2 ($p < 0.001$), in which LL_{300} was higher than in other groups ($p < 0.001$). Both LL_1 and DD were higher than SCNx ($p < 0.001$).

$^{low}PSD_{we}$ analysis produced negative β slope values, which demonstrated the 1/f fGn noise in all groups (Table 1). The 2-way ANOVA analysis for stage, group, and their interaction revealed significant results ($p < 0.05$, $p < 0.001$, and $p < 0.001$, respectively). Specific effects for stage were found only in the SCNx group ($p < 0.001$). Groups were statistically different within s_2 ($p < 0.001$); the highest values found were for LL_{300}, $LL_{1.3}$, and DD compared to SCNx ($p < 0.001$).

DISCUSSION

Here, we studied the motor activity patterns of rats exhibiting behavioral arrhythmicity, with the aim to demonstrate the involvement of the SCN in the regulation of activity patterns in the short time scale and the ultradian range. The Hurst index depended on the presence of SCN regulation and light intensity. Our results indicate the role played by SCN in causing time correlations in short time scales (around 1 h). Our results also show that in nonlesioned rats, this role appears to be independent of the SCN circadian output because following the loss of functional circadian regulation (LL), the time correlation was sustained and modulated by light. Thus, the dynamics of time correlation must be related to the light intensity used.

The main ultradian frequencies (periods from 8 h to 4 h) were observed in intact rats with arrhythmicity under LL conditions. Because SCNx animals did not show ultradian components, it is possible that SCN activity is responsible for the ultradian pattern, as suggested by Hu et al. (2007). The present work also shows that ultradian components in arrhythmic rats were higher under LL_{300} conditions than $LL_{1.3}$. Theoretically, there are 2 possible explanations for the emergence of ultradian components: 1) a single frequency process with a stable phase (producing a peak in the spectra), and 2) multiple circadian oscillators with intrinsically different periods, the phases of which are unevenly distributed throughout the day.

In this study, both LL groups showed ultradian components in the serial Fourier analyses (Figure 2A), although this was not the case in the global periodogram (Figure 1). This clearly indicates the presence of ultradian components within each day but with a day-to-day phase instability. This could indicate that they are not attributable to a single ultradian process. The second theory is therefore more plausible. It is important to differentiate between 2 types of circadian activity in the SCN: one at the cellular level, whereby each oscillator exhibits a circadian rhythm, and the other type of activity is found at the general (tissue) level, whereby oscillators are synchronized.

The SCN tissue is composed of a network of cell-autonomous neuronal oscillators, whereby the periods are distributed throughout a 24-h period (Welsh et al., 1995; Herzog et al., 1998). A regulatory role of light in SCN network interactions (coupling) has been suggested by various authors (Díez-Noguera, 1994; Honma and Honma, 1999; Quintero et al., 2003).

In the present study, we confirm that scale-invariant motor patterns were immediately abolished by SCNx, which was previously demonstrated by Hu et al. (2007). Arrhythmicity in SCNx animals resulted in a flattened spectrum together with uncorrelated (random) noise, which was sustained in time. Because random noise prevailed in SCNx motor activity output, we can interpret the noise as the read-out of a large number of nonlinear interactions, coming downstream along the SCN from motor neural effectors. In addition, we have demonstrated that *H* values show stable scale-invariant patterns under normal circadian regulation under DD conditions.

However, it is important to note that in contrast with results found for the SCNx-elicited arrhythmicity, rats that became arrhythmic under LL conditions maintained scalar time correlation, even when the circadian activity was disrupted. This indicates that although the fractal SCN regulation overlays circadian rhythmicity, it can be separated from the circadian output under LL conditions. Indeed, it has been reported that observed differences in the amount of fractal noise may indicate different degrees of interactions between underlying physiological processes (Eke et al., 2002).

The mechanism by which LL produces arrhythmicity is not yet completely understood. After 50 days in LL, PER2 protein levels were constantly elevated throughout the cycle, suggesting that light might act, inhibiting some mechanisms that normally degrade *mPer2* (Muñoz et al, 2005). On the other hand, monitoring *Per1* within individual SCN neurons revealed that the rhythm disruption is due to desynchrony among neurons that sustain circadian oscillation (Ohta et al., 2005). Additionally, several experimental models have pointed to a SCN multioscillator regulation of motor output in the rat (Nakamura et al., 2001; de la Iglesia et al., 2004). Thus, ultradian activity may result in an emergent pattern of desynchronized circadian oscillators, showing a given degree of coupling based on lighting conditions. However, the circadian system is actually more complex than a network of oscillators in the SCN because it also includes the interaction with other peripheral oscillators (Schibler, 2009). Thus, interaction of the SCN with other non-SCN neuronal sites receiving light input must also be considered. For instance, neuronal oscillators in the retina interact continuously with the SCN to determine the free-running period, but not rhythmicity, of locomotor activity (Yamazaki et al., 2002). It could be that the fractal correlation would be altered by the disruption between the SCN and other non-SCN neuronal sites. Moreover, we cannot disregard that other mechanisms related with light perception in the animal may also be responsible for the scale invariance properties. We do not know the extent of damage in the optic chiasm due to the lesions, which could produce that this group received less amount of light, making it different from the rest of the animals.

We believe that the results of our experiment can be better explained in terms of constant light reducing the degree of coupling between the population of oscillators. We can suppose that, under constant bright light, the interactions between the oscillators should be reduced, leaving the oscillators to run relatively undisturbed by the influence of their neighbors, and consequently, the behavior of each oscillator should be rather predictable. This could explain why the fractal analysis revealed high time correlation (predictability) under LL_{300}, while motor patterns under $LL_{1.3}$ and DD showed lower correlation values.

In the case of DD, we can assume that because strong interactions between oscillators are present, due to a high degree of coupling, that the behavior of each oscillator is less predictable (more chaotic) because it is strongly influenced by others. This explains why *H* had the lowest values under DD conditions. $LL_{1.3}$ showed intermediate values of *H*, which could be because the coupling among the oscillators should be between the other 2 groups. It is also apparent in LL_{300} and $LL_{1.3}$ that although the system showed a circadian rhythm under s_1 and not under either s_2 or the other stages, *H* did not change between s_1 and s_2, indicating the same oscillator interactions in both stages. Thus, fractal structure is due to the interaction between the network of circadian oscillator that affects the functioning of each individual oscillator. Although most of our results and literature evidence seem to favor the short-term regulation of motor activity produced by the network properties among the oscillators in the SCN, we cannot forget that light may act directly or indirectly in other structures of the circadian system.

We can therefore speculate that the circadian rhythm in s_1 occurs when the interaction between the oscillators is very low, due to the inhibiting coupling effect of light; however, due to the oscillators' inertia, their phases are still not spread. It is also remarkable that, although *H* values are sustained in the LL_{300} group, and in the DD group, they decrease over time in group $LL_{1.3}$. We suggest that in a state of intermediate coupling, the coupling among oscillators may increase slightly over time, and thus, their functionality becomes less predictable. Indeed, under LL conditions, s_1 actually corresponds to a transient state, whereby the oscillators are still in phase but already with low coupling. Although absent from our assessment, the duration of the transient stage could provide information about the inertia of the oscillators.

The fractal nature of ultradian rhythms has been discussed previously with regard to the activity of the SCN pacemaker (Lloyd and Lloyd, 1993) and more generally in other biological systems (Losa et al., 1997; Brodsky, 2006). On one hand, to produce scale-invariant patterns from multiple ultradian

fluctuations, a scalar distribution of amplitudes must be generated by such activity, which is statistically unlikely if these oscillations are independent (pointing to uncoupled circadian oscillators). However, we found that the *H* coefficient featured a time-dependent process below 1 h (t_c), which did not seem to be related to ultradian components, as has been previously suggested for human activity (Hu et al., 2004). Indeed, ultradian regulation below 2.6 h was not observed in this work.

The aim of the fractal approach was to demonstrate the presence of scale-invariant features (i.e., internal correlation or memory) in a detailed record of temporal variations of a physiological parameter (Eke et al., 2002). Moreover, previous simulations have indicated that rather than simple superposition of independent controlling factors (Hausdorff and Peng, 1996), temporal scale invariance can be generated by a network of feedback interactions among control nodes that operate along different time scales (Bak et al., 1987; Basu et al., 2004). Thus, a fractal analysis could be useful in understanding the complexity of physiological functions, particularly in this work for studying SCN output regulation.

In summary, we analyzed both the ultradian and the short time scale regulation characterizing motor activity patterns. A useful framework was designed by studying such patterns under different circadian conditions. The following conclusions can be drawn: 1) the presence of the SCN is important for the short time range regulation of motor activity; 2) rather than stochastic, arrhythmic patterns under LL, conditions maintain a temporal structure, both at the ultradian frequencies and along short time scales (~1 h); 3) scale-invariant regulation seems to depend on the light intensity modulation of the SCN activity but is independent of the circadian output; and 4) the degree of interaction between the oscillatory elements of the SCN could be involved in this modulation process, modifying the spontaneous, predictable function of the single oscillators.

ACKNOWLEDGMENTS

This study was supported by the Ministerio de Ciencia y Tecnología, Spain, with projects BFU2008-00199 and PCI2005-A7-0470. Juan J. Chiesa is a researcher from the National Council of Science and Technology, CONICET, Argentine. The authors thank Dr. Jordi Garcia-Ojalvo for useful comments on the article.

REFERENCES

Antle MC and Silver R (2005) Orchestrating time: arrangements of the brain circadian clock. Trends Neurosci 28:145-151.

Bak P, Tang C, and Wiesenfeld K (1987) Self-organized criticality: an explanation of the 1/f noise. Phys Rev Lett 59:381-384.

Basu S, Foufoula-Georgiou E, and Porte-Agel F (2004) Synthetic turbulence, fractal interpolation, and large-eddy simulation. Phys Rev E Stat Nonlin Soft Matter Phys 70:026310.

Brodsky VY (2006) Direct cell-cell communication: a new approach derived from recent data on the nature and self-organization of ultradian (circahoralian) intracellular rhythms. Biol Rev Camb Philos Soc 81:143-162.

de la Iglesia HO, Cambras T, Schwartz WJ, and Díez-Noguera A (2004) Forced desynchronization of dual circadian oscillators within the rat suprachiasmatic nucleus. Curr Biol 14:796-800.

Delignieres D, Ramdani S, Lemoine L, Torre K, Fortes M, and Ninot G (2006) Fractal analyses for 'short' time series: a re-assessment of classical methods. J Math Psychol 50:522-544.

Deprés-Brummer P, Lévi F, Metzger G, and Touitou Y (1995) Light-induced suppression of the rat circadian system. Am J Physiol 268:R1111-R1116.

Díez-Noguera A (1994) A functional model of the circadian system based on the degree of intercommunication in a complex system. Am J Physiol 267:R1118-R1135.

Eastman C and Rechtschaffen A (1983) Circadian temperature and wake rhythms of rats exposed to prolonged continuous illumination. Physiol Behav 31:417-427.

Eastman CI, Mistlberger RE, and Rechtschaffen A (1984) Suprachiasmatic nuclei lesions eliminate circadian temperature and sleep rhythms in the rat. Physiol Behav 32:357-368.

Eke A, Hermán P, Bassingthwaighte JB, Raymond GM, Percival DB, Cannon M, Balla I, and Ikrényi C (2000) Physiological time series: distinguishing fractal noises from motions. Pflugers Arch 439:403-415.

Eke A, Herman P, Kocsis L, and Kozak LR (2002) Fractal characterization of complexity in temporal physiological signals. Physiol Meas 23:R1-R38.

Fadel PJ, Barman SM, Phillips SW, and Gebber GL (2004) Fractal fluctuations in human respiration. J Appl Physiol 97:2056-2064.

Goldberger AL, Amaral LA, Hausdorff JM, Ivanov PCh, Peng CK, and Stanley HE (2002) Fractal dynamics in physiology: alterations with disease and aging. Proc Natl Acad Sci U S A 99:2466-2472.

Hausdorff JM and Peng CK (1996) Multiscaled randomness: a possible source of 1/f noise in biology. Phys Rev E Stat Phys Plasmas Fluids Relat Interdiscip Topics 54:2154-2157.

Herzog ED, Takahashi JS, and Block GD (1998) Clock controls circadian period in isolated suprachiasmatic nucleus neurons. Nat Neurosci 1:708-713.

Honma S and Honma K (1999) Light-induced uncoupling of multioscillatory circadian system in a diurnal rodent, Asian chipmunk. Am J Physiol Regul Integr Comp Physiol 276:R1390-R1396.

Hu K, Ivanov PCh, Chen Z, Hilton MF, Stanley HE, and Shea SA (2004) Non-random fluctuations and multi-scale dynamics regulation of human activity. Physica A 337:307-318.

Hu K, Scheer FA, Buijs RM, and Shea SA (2008) The endogenous circadian pacemaker imparts a scale-invariant pattern of heart rate fluctuations across time scales spanning minutes to 24 hours. J Biol Rhythms 23:265-273.

Hu K, Scheer FA, Ivanov PC, Buijs RM, and Shea SA (2007) The suprachiasmatic nucleus functions beyond circadian rhythm generation. Neuroscience 149:508-517.

Leak RK and Moore RY (2001) Topographic organization of suprachiasmatic nucleus projection neurons. J Comp Neurol 433:312-334.

Lloyd AL and Lloyd D (1993) Hypothesis: the central oscillator of the circadian clock is a controlled chaotic attractor. BioSystem 29:77-85.

Long MA, Jutras MJ, Connors BW, and Burwell RD (2005) Electrical synapses coordinate activity in the suprachiasmatic nucleus. Nat Neurosci 8:61-66.

Losa GA, Merlini D, Nonnenmacker TF, and Weibel ER (1997) *Fractals in Biology and Medicine II*. Basel, Birkhauser.

Maywood ES, Reddy AB, Wong GK, O'Neill JS, O'Brien JA, McMahon DG, Harmar AJ, Okamura H, and Hastings MH (2006) Synchronization and maintenance of timekeeping in suprachiasmatic circadian clock cells by neuropeptidergic signaling. Curr Biol 16:599-605.

Moore RY, Speh JC, and Leak RK (2002) Suprachiasmatic nucleus organization. Cell Tissue Res 309:89-98.

Muñoz M, Peirson SN, Hankings MW, and Foster RG (2005) Long-term constant light induces constitutive elevated expression of mPER2 protein in the murine SCN: a molecular basis for Aschoff's rule? J Biol Rhythms 20:3-14.

Nakamura W, Honma S, Shirakawa T, and Honma K (2001) Regional pacemakers composed of multiple oscillator neurons in the rat suprachiasmatic nucleus. Eur J Neurosci 14(4):666-674.

Ohta H, Yamazaki S, and McMahon DG (2005) Constant light desynchronizes mammalian clock neurons. Nat Neurosci 8:267-269.

Paxinos G and Watson C (1998) *The Rat Brain in Stereotaxic Coordinates*. New York, Academic Press.

Peng CK, Havlin S, Hausdorff JM, Mietus JE, Stanley HE, and Goldberger AL (1995) Fractal mechanisms and heart rate dynamics: long-range correlations and their breakdown with disease. J Electrocardiol 28:59-65.

Pittendrigh CS (1981a) Circadian systems: entrainment. In *Handbook of Behavioural Neurobiology: Biological Rhythms*, Aschoff J, ed, pp 95-124, New York, Plenum Press.

Pittendrigh CS (1981b) Circadian systems: general perspective. In *Handbook of Behavioural Neurobiology: Biological Rhythms*, Aschoff J, ed, pp 57-80, New York, Plenum Press.

Quintero JE, Kuhlman SJ, and McMahon DG (2003) The biological clock nucleus: a multiphasic oscillator network regulated by light. J Neurosci 23:8070-8076.

Schibler U (2009) The 2008 Pittendrigh/Aschoff lecture: peripheral phase coordination in the mammalian circadian timing system. J Biol Rhythms 24:3-15.

Sokolove PG and Bushell WN (1978) A chi square periodogram: its utility for the analysis of circadian rhythms. J Theor Biol 72:131-160.

Steinlechner S, Stieglitz A, and Ruf T (2002) Djungarian hamsters: a species with a labile circadian pacemaker? Arrhythmicity under a light-dark cycle induced by short light pulses. J Biol Rhythms 17:248-258.

Stephan FK and Zucker I (1972) Circadian rhythms in drinking behavior and locomotor activity of rats are eliminated by hypothalamic lesions. Proc Natl Acad Sci USA 69:1583-1586.

van Beek JH, Roger SA, and Bassingthwaigthe JB (1989) Regional myocardial flow heterogeneity explained with fractal networks. Am J Physiol 257:H1670-H1680.

Welsh DK, Logothetis DE, Meister M, and Reppert SM (1995) Individual neurons dissociated from rat suprachiasmatic nucleus express independently phased circadian firing rhythms. Neuron 14:697-706.

Winfree AT (1971) Corkscrews and singularities in fruitflies: resetting behavior of the circadian eclosion rhythm. In *Biochronometry*, Menaker M, ed, pp 81-109, Washington DC, National Academy of Sciences.

Yamaguchi S, Isejima H, Matsuo T, Okura R, Yagita K, Kobayashi M, and Okamura H (2003) Synchronization of cellular clocks in the suprachiasmatic nucleus. Science 302(5649):1408-1412.

Yamazaki S, Alones V, and Menaker M (2002) Interaction of the retina with suprachiasmatic pacemakers in the control of circadian behavior. J Biol Rhythms 17(4):315-329.